

Preferred frequencies for three unconsolidated earth materials

Laura E. Gilcrist^{a)}

Department of Geology, State University of New York at Buffalo, Buffalo, New York 14260, USA

Gregory S. Baker

Department of Earth and Planetary Science, University of Tennessee, Knoxville, Tennessee 37996, USA

Surajit Sen

Department of Physics, State University of New York at Buffalo, Buffalo, New York 14260, USA

(Received 1 June 2007; accepted 12 November 2007; published online 17 December 2007)

Exploring near-surface mechanical wave propagation through cohesive and noncohesive soils is important for detecting buried objects (i.e., landmines and unexploded ordnance). Here, we determine that certain *preferred frequencies* travel through specific soils more efficiently. A controlled-frequency acoustic seismic source was developed to modulate the applied frequency and amplitude. Surface response due to continuous waves traveling through soils was recorded both instantaneously and after a finite load time. Preferred frequencies for sand, clay loam, and silt loam were measured to be 300–330, 100–140, and 140–260 Hz, respectively. Observed frequency shifts were dependent upon applied amplitude and load time. © 2007 American Institute of Physics. [DOI: 10.1063/1.2820606]

Mechanical wave propagation through earth materials has long been studied and used to detect oil reservoirs, the water table, and buried objects such as barrels and archaeological artifacts.^{1,2} Recently, scientists have used mechanical waves to explore the Earth's upper 2 m.³ These studies indicate that surficial soils are highly complex systems and behave differently than compressed earth materials found at greater depths.^{4–9} Specifically, acoustic wave propagation through near surface Earth materials is known to behave nonlinearly, with a dependence upon soil moisture, soil type, and amplitude.^{2,4–8,10–15} A deeper insight into the role of mechanical wave propagation may allow objects buried near the Earth's surface to be detected and identified more accurately and efficiently.^{2,16} Increased understanding may also complement research in other near-surface processes such as land sliding and biological phenomena.^{17,18}

To explore mechanical wave propagation within the upper 1 m, data were collected in sand, clay loam, and silt loam using standard near-surface seismic equipment in conjunction with a controlled-frequency acoustic seismic source (CASS). The CASS allows for isolation and modulation of the source signal frequency (60–1000 Hz), amplitude (5 and 10 V p.p.), and load time (0, 5, and 10 s). Recording successive iterations while altering only one variable at a time yielded approximately 140 different initial source conditions at each site each, with a total of approximately 400 different conditions. Soil temperatures were 10, 14, and 11 °C (± 0.5 °C during the experiments), air temperatures were 6.6, 13.8, and 10.4 °C (± 1.5 °C during the experiments), and soil moisture was 7.1%, 2.7%, and 3.3% for the sand, clay loam, and silt loam, respectively.⁹

The CASS is not necessarily intended to replace current seismic sources, but rather to allow consistent waveform control.^{16–19} The CASS is composed of a Good Will Instek 15 MHz Programmable Function Generator powered by a 12 V battery via dc to ac power inverter. The function gen-

erator is connected to both a Pioneer 240 W speaker and a Geometrics R-60 StrataView seismograph. This three-way connection allows the function generator to trigger the speaker and seismograph simultaneously. Receivers consist of 60 L40A 40 Hz Mark Products geophones with 7.75 cm ground spike that measure the rate (velocity) of ground motion (in volts). The 60 geophones are planted 10 cm apart, creating a 5.9 m surface profile. The recording time, sampling interval, and stack for each geophone are 256 ms, 0.03125 ms, and three files, respectively (stack is defined as the number of files summed to create a single file). The CASS is located in the middle of a linear profile (“split spread”) for all cases [Fig. 1(a)].

Once data are collected, survey geometry is entered and data is viewed using seismic processing workshop (by Parallel Geosciences Incorporated). Raw data in the time domain is converted to the frequency domain using a Fourier analysis. For each set of initial conditions an amplitude spectrum is generated [Fig. 1(b)]. Each amplitude spectrum has a maximum value with coordinates (x, y) or (frequency, amplitude). The amplitude (y coordinate) associated with the maximum value is referred to as the “received maximum amplitude,” or RMA [Fig. 1(c)]. The frequency (x coordinate) associated with the maximum value is referred to as the “received maximum amplitude frequency,” or RMAF [Figure 1(d)]. Both the RMA and the RMAF are plotted against the applied frequency resulting in two graphs for each set of initial conditions: (1) the RMA for each amplitude spectra versus the applied frequency, ranging from 60 to 1000 Hz [Fig. 1(c)], and (2) the RMAF for each amplitude spectra versus the applied frequency, ranging from 60–1000 Hz [Fig. 1(d)].

The RMA graphs indicate that there are applied frequencies which yield the largest received maximum amplitudes; these are called *preferred frequencies*. The RMAF graphs show a range of frequencies for which the applied frequency is equivalent to the received frequency with the greatest maximum amplitude. This phenomena is referred to as *frequency equivalence*. To compare data between soil types,

^{a)}Electronic mail: leg4@buffalo.edu.

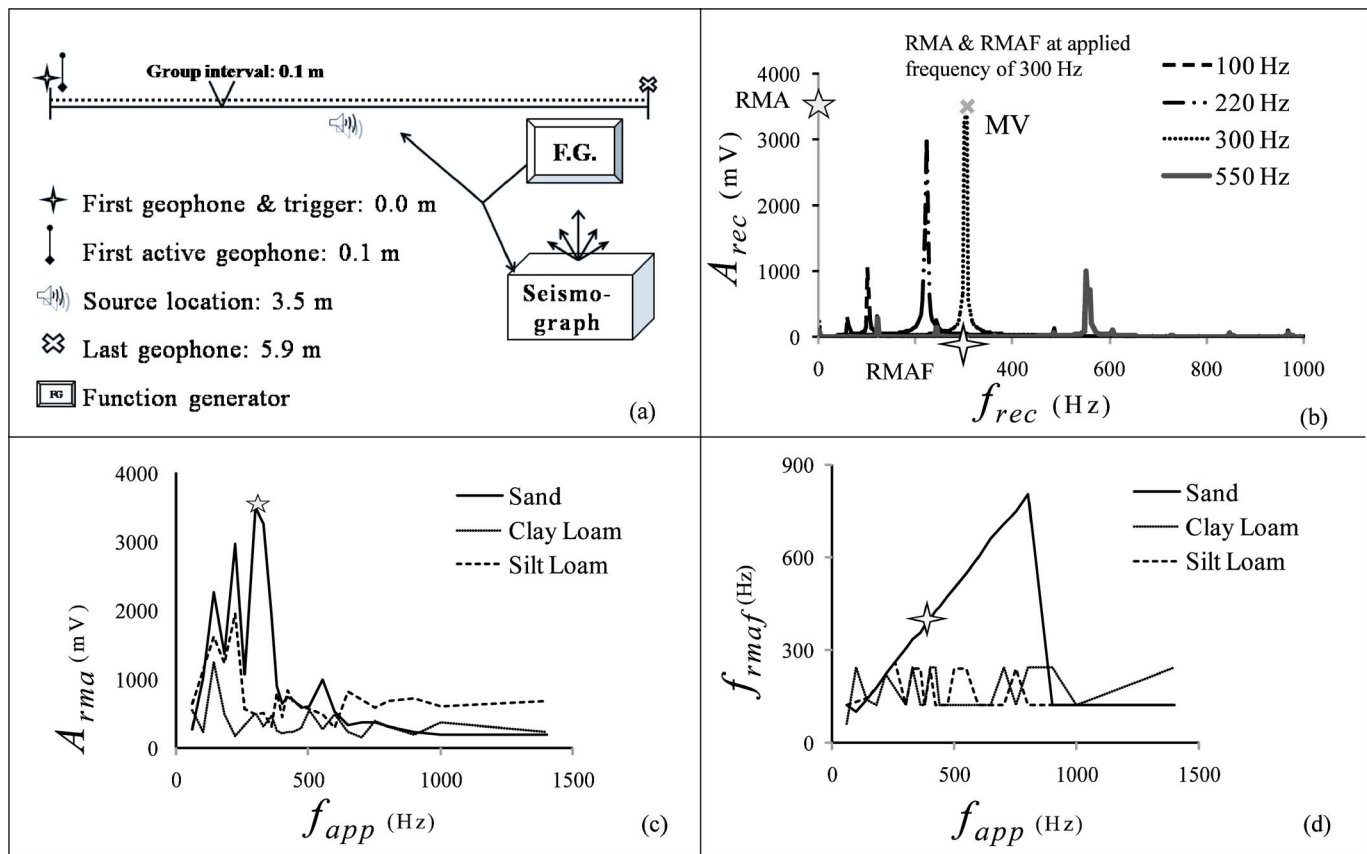


FIG. 1. (Color online) (a) Schematic of survey design. The speaker, seismograph, and function generator are connected together using a three-way BNC connection. This ensures simultaneous triggering of the seismograph and speaker. (b) The amplitude spectra of data collected with no forcing function. MV is the maximum value for the amplitude spectra at an applied frequency of 300 Hz. MV has coordinates (x, y) where x is the RMAF and y is the RMA. (c) Shows the RMA, A_{RMA} , for each site as a function of the applied frequency. (d) Shows the RMAF, f_{RMAF} , for each site as a function of applied frequency. For both (c) and (d) the value located at 1500 Hz is associated with noise.

frequency equivalence (FE) is expressed as a percentage (FE%) and a range (FER), where the frequency-equivalence range is defined to be the range of frequencies for which frequency equivalence occurs. Both the frequency-equivalence percent and range are determined for each change in frequency, amplitude, load time, and soil type.

The RMA and RMAF graphs show that the preferred frequencies for sand, clay loam, and silt loam are 300–330, 100–140, and 140–260 Hz, respectively (see Table I). The FE% and FER for sand, clay loam, and silt loam are 70%–91% and 60–1000 Hz, 13%–32% and 60–360 Hz, and 9%–40% and 60–550 Hz (see Table II). The variance at each site is dependent upon the initial amplitude and load time. Table I shows that the RMAF for sand and clay loam is stable at 300 and 140 Hz, respectively, with a shift for sand to 330 Hz (at 5 V p.p. applied amplitude and 0 s load time), and a shift

for clay loam to 100 Hz (at 5 V p.p. applied amplitude and 10 s load time). This contrasts with the RMAF stability in silt loam which has four different RMAF's dependent upon initial conditions.

Sand has a consistently high FE%, 70%–91%, and a large FER, 60–1000 Hz, for all applied amplitudes and load times (see Table II). The applied frequency is equal to the RMAF independent of initial amplitude and load time, indicating that sand grains will oscillate over a large range of frequencies without regard to other parameters. Therefore, frequency is a highly effective controlling variable in the grain dynamics of sand and demonstrates a linear relationship.

Clay loam has a low FE%, 13%–32%, and range, 60–360 Hz (see Table II). This suggests that only a small number of applied frequencies will result in frequency

TABLE I. The RMA, RMAF (mV, Hz) for a fixed initial soil, amplitude, and load time (given). The frequency is modulated from 60–1000 Hz.

Soil	Sand	Clay Loam	Silt Loam
10 V p.p., 0 s	(3495, 300)	(1254, 140)	(1959, 220)
5 V p.p., 0 s	(2203, 330)	(1298, 140)	(2065, 140)
10 V p.p., 5 s	(6399, 300)	(858, 140)	(3630, 140)
5 V p.p., 5 s	(3112, 300)	(1045, 140)	(609, 260)
10 V p.p., 10 s	(9322, 300)	(2782, 140)	(4195, 180)
5 V p.p., 10 s	(2434, 300)	(775, 100)	(1334, 140)

TABLE II. The frequency-equivalence percentage and the frequency-equivalence range (R) for fixed initial soil type, applied amplitude, and load time. Frequency was modulated from 60–1000 Hz. P indicates the projected number which is given when applied frequencies are missing from the data set, which are given by M .

Soil	Sand	Clay Loam	Silt Loam
10 V p.p., 0 s	87%, R 100–800	14%, P : 17%, R : 60, 140, 220, M : 260	18%, R : 140–260
5 V p.p., 0 s	83%, R : 60–180, 260–700	32%, R : 60–300	26%, R : 100–260, 440
10 V p.p., 5 s	91%, R : 100–800, 1000	22%, R : 60–180, 260	40%, R : 60–220, 380, 420, 550
5 V p.p., 5 s	75%, P : 78% R : 100–700, M : 60, 400, 440, 470	17%, R : 100, 140, 360, 600	9%, R : 100–180
10 V p.p., 10 s	91%, P : 91% R : 100–900, M : 140	18%, P : 17%, R : 60–180, M : 420	32%, R : 100–260, 380, 800
5 V p.p., 10 s	70%, R : 100–300, 360, 380, 420–550, 650, 700, 1000	13%, R : 100–180	22%, R : 100–220, 300

equivalence. Waves propagating through clay loam at initial high frequencies cannot be sustained and quickly break down into lower frequency waves. This indicates that the natural frequency of clay loam has a stronger effect on grain dynamics than the initial frequencies when greater than ~ 360 Hz. The frequency parameter in clay loam grain dynamics is predictable in that it demonstrates a linear dependence between applied frequencies of ~ 60 –300 Hz and a nonlinear dependence between applied frequencies of ~ 300 –1000 Hz.

Silt loam has a low FE%, 9%–40%, but a high range, 60–550 Hz (see Table II). Thus, the frequency equivalence is uncommon and difficult to predict. This also indicates that the grain dynamics in silt loam has a complex and possibly strongly dissipative nonlinear response.

Frequency-equivalence results are consistent with results by Goldin *et al.*²⁰ and agree with elastic moduli predictions, where low moduli soils cause high attenuation (clay loam and silt loam), and high moduli soil cause low attenuation (sand).

Results indicate that heterogeneous soils have preferred frequencies dependent upon soil type and initial wave conditions. Preferred frequencies result in the largest received amplitudes, increasing the recorded signal and, thus, causing individual grains (or coherent clumps of grains) to oscillate at their greatest amplitudes before frictional and damping forces cause wave destruction. The preferred frequencies in complex soil systems studied here are analogous to resonant frequencies in linear acoustics. We suspect that these are dominant collective grain vibration frequencies, and a further increase in the frequency will exceed a threshold beyond which damping effects are likely to dominate.

Preferred frequency shifts dependent upon amplitude reveals the nonlinear behavior of near surface soils. Observed shifts are explained by the elastic modulus of soil which is changes in response to varying the applied mechanical wave form; exhibiting nonlinear behavior.^{21,22} To investigate the nonlinear nature of wave speed in soil an additional experiment was conducted where amplitudes of 2.5, 5, 7.5, and 10 V p.p. were applied. Signal time of flight was used to determine wave velocity. Results show velocity changes with

amplitude and frequency; this dependence confirms that acoustic propagation in soil is nonlinear.¹⁰

In addition to the impact of these results on detection methods for landmines, findings have implications for near-surface seismic reflection surveys, landslide and slope stability studies, and models of wave propagation through soil.

This research was partially funded by grants from the NSF INT-0243524, NSF GEO-0119871, the Jones/Bibee Geophysics Endowment at the University of Tennessee (GSB), and by ARO (SS).

¹W. E. Doll, R. D. Miller, and J. Xia, *Geophysics* **63**, 1318 (1998).

²Y. Q. Zeng and H. L. Qing, *IEEE Trans. Geosci. Remote Sens.* **39**, 1165 (2001).

³G. S. Baker, D. W. Steeples, and C. Schmeissner, *Geophysics* **64**, 323 (1998).

⁴G. S. Baker, D. W. Steeples, and C. Schmeissner, *First Break* **20**, 35 (2002).

⁵M. A. Biot, *J. Acoust. Soc. Am.* **28**, 168 (1956).

⁶M. A. Biot, *J. Acoust. Soc. Am.* **28**, 179 (1956).

⁷M. A. Biot, *J. Appl. Phys.* **33**, 1482 (1962).

⁸T. Flammer, A. Blum, A. Leiser, and P. Germann, *J. Appl. Geophys.* **46**, 115 (2001).

⁹W. H. Gardner, *Agron. J.* **9**, 493 (1986).

¹⁰S. Sen, T. R. K. Mohan, D. Visco, S. Swaminathan, A. Sokolow, E. Avalos, and M. Nakagawa, *Int. J. Mod. Phys. B* **18**, 2951 (2005).

¹¹D. Visco, Jr., S. Swaminathan, K. Mohan, A. Sokolow, and S. Sen, *Phys. Rev. E* **70**, 051306 (2004).

¹²M. Scalerandi, V. Agostini, and P. P. Delsanto, *J. Acoust. Soc. Am.* **113**, 3049 (2003).

¹³S. Sen, M. Manciu, R. S. Sinkovits, and A. J. Hurd, *Granular Matter* **3**, 33 (2001).

¹⁴R. S. Sinkovits and S. Sen, *Phys. Rev. Lett.* **74**, 2686 (1995).

¹⁵S. Swaminathan, D. P. Visco, Jr., and S. Sen, *Appl. Phys. Lett.* **90**, 154107 (2007).

¹⁶J. K. Schrodt, *Geophysics* **52**, 469 (1987).

¹⁷J. T. Botz, C. Loudon, J. B. Barger, J. S. Olafsen, and D. W. Steeples, *Integr. Comp. Biol.* **42**, 6 (2002).

¹⁸R. V. Ghose, V. Nijhof, J. Brouwer, Y. Matsubara, Y. Kaida, and T. Takahashi, *Geophysics* **63**, 1295 (1998).

¹⁹S. S. Haines, *J. Environ. Eng. Geophys.* **11**, 9 (2006).

²⁰S. V. Goldin, Y. I. Kolesnikov, and S. V. Polozov, *Phys. Mesomech.* **2**, 97 (1999).

²¹Z. Lu, *J. Acoust. Soc. Am.* **120**, 3281 (2006).

²²L. A. Ostrovsky and P. A. Johnson, *Riv. Nuovo Cimento* **24**, 7 (2001).